JOURNAL OF MATERIALS SCIENCE 20 (1985) 193–198

On the size distribution of small regular fragments

Y. GUR, R. ENGLMAN, Z. JAEGER
Soreq Nuclear Research Centre, Yavne 70600, Israel

Two- and three-dimensional small-sized fragments in solids are modelled by rectangular parallelograms and parallelopipeds formed of randomly distributed "cracks", namely, lines or plaquettes of constant size. Size and shape distributions are derived for the fragments and it is shown that the cumulative size distribution function is usefully represented by the "Mott distribution" (an exponential decrease with the linear size of the fragment). For increasing size, upward and downward deviations from this distribution occur for high and low crack densities, respectively.

1. Introduction

In several branches of mineral processing the size distribution of rock-pieces is a technologically and economically important factor. Thus in the burning of oil-shale one desires to have a fairly narrow range of fragment sizes. Especially problematic are the small pieces (so-called "fines", of diameter less than 1.5 cm) since these tend to smother the combustion or to leave the processing plant through the chimney. In an ambitious design of the plant, one would even need the distribution of fines, not just their total number, so as to take into account their thermo- and aerodynamic properties.

Experimental determinations of rock-size distributions have been undertaken [1, 2] and, as a result, empirical laws have been proposed for the number of rock-pieces as a function of fragment-size. The laws include Poisson distribution with respect to the linear dimension of the piece (the so-called Mott distribution) [3], a generalization of this [4], a log normal distribution [1, 5], and others [6]. Some theoretical justification has been presented for the Mott distribution [7].

Stereological approaches to the problem in two dimensions have considered the distribution of areas formed by infinitely long lines [8]. For two sets of lines with a fixed angle, ϕ, between them, and each set having a mean separation, λ^{-1}, between the lines, formulae can be given for $f^{\infty}(a)$ the distribution of areas (a) or the cumulative fraction, this being defined as the fraction of areas with sizes larger than a [3]. Explicitly [9]

$$f^{\infty}(a) = 2\lambda^2 \sin\phi K_0 [2\lambda(a \sin\phi)^{\frac{1}{2}}]$$

where K_0 is a Bessel function.

For infinite lines with arbitrary orientation the first and second moments have been given but not the distribution ([8], Ch. 3).

This work aims at the statistics of small rectangular parallelograms (Fig. 1) and parallelopipeds (Fig. 2) (collectively called small regular fragments) formed by boundaries (lines or square plaquettes) of fixed dimensions (L or L^2) oriented along two or three orthogonal directions. As noted above, consideration of small fragments is justified by their technological significance. Moreover, it will be argued that the majority of small fragments will be the regular ones, namely those formed by four lines or by six plaquettes, rather than irregular ones which are bounded by a larger number of boundaries.

2. The model

2.1. Plaquettes

A model of "plaquettes" is used to obtain the distribution of fragments in three dimensions ($d = 3$). The simpler and less realistic case of two dimensions ($d = 2$) will be given incidentally. It is known that fragments are formed by cracks surrounding the rock-piece, whereas cracks arise during a typical dynamic process (such as explo-

0022–2461/85 $03.00 + .12

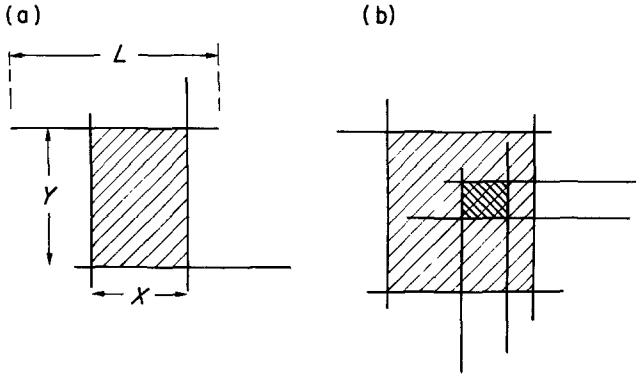

Figure 1 Small regular fragments in a plane. (a) A fragment (shaded) in the form of a perpendicular parallelogram with edges X, Y formed by orthogonal lines of length L. (b) Two regular fragments are shown with different shadings. The area of the small fragment is also included in the larger fragment.

sive fracture) in a way which is not far from random. The situation is simplified by postulating three types of plaquettes, oriented in three orthogonal directions, i.e. having normals along x, y and z, respectively. Plaquettes are square and of equal size ($L \times L$); each type is randomly distributed in space with a density, ρ. The plaquette model has been used for a discrete lattice by Aizenman *et al.* [10] in a study of phase transitions and a two-dimensional form of it by Robinson [11] to investigate percolation.

The present research is concerned with rectangular parallelopipeds (abbreviated PPP) formed by six plaquettes and seeks the number of PPP as functions of their volume, v, shapes, etc, as well as of the dimensionless density, $\rho' = \rho L^3$. Admittedly, fragments (i.e. three-dimensional forms) of other, more complex shapes than PPP will also be present. However, it is believed that the small-sized fragments ($\ll L^3$) are made up predominantly from PPP, other shapes being characteristically of larger size. (This belief is to some extent substantiated by photographs of crushed rock in which small pieces tend to have simple shapes and large ones are jugged [12].) We return to this point later.

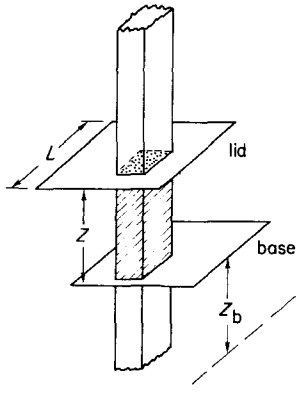

Figure 2 Construction of a rectangular parallelopiped (shaded) from a long hollow column and two square plaquettes (base and lid) placed a distance Z apart. A section of the column is shown dotted.

2.2. Derivation of the distribution

In any event the distribution of PPP is a well-defined problem which can be approached by a combination of probabilistic and computational methods. Define $N(X, Y, Z)\mathrm{d}X\mathrm{d}Y\mathrm{d}Z$ as the number of PPP in a large volume ($\gg L^3$) having edge lengths in the intervals $(X - \mathrm{d}X, X)$, $(Y - \mathrm{d}Y, Y)$ and $(Z - \mathrm{d}Z, Z)$. Consider now a long hollow rectangular column of sides X, Y and length $V^{1/3}$. From a PPP by inserting a "base" and a "lid" (Fig. 2). Suppose that the basal plaquette is at a point Z_b along the column: then the conditional probability for the nearest plaquette (the lid, that fully covers the cross-section of the column) to be in the interval $(Z_b + Z - \mathrm{d}Z, Z_b + Z)$ is:

$$\rho[(L-X)(L-Y)]e^{-\rho[(L-X)(L-Y)]Z}\mathrm{d}Z \quad (1)$$

where the quantity $(L-X)(L-Y)$ is the area on which a fixed point on the plaquette (e.g. its centre) must lie in order to fully cover the cross-section [8]. The number of basal plane fully containing the cross section is:

$$V^{1/3}\rho(L-X)(L-Y)$$

Applying similar considerations to the sides in the X and Y directions yields the number of PPP in the volume, V:

$$\begin{aligned} &N(X, Y, Z)\mathrm{d}X\mathrm{d}Y\mathrm{d}Z \\ &\quad = V\rho^6[(L-X)(L-Y)(L-Z)]^4 \\ &\qquad \times \exp\{-\rho[L^2(X+Y+Z) \\ &\qquad - 2L(XY+YZ+ZX) + 3XYZ]\}\mathrm{d}X\mathrm{d}Y\mathrm{d}Z \end{aligned} \quad (2)$$

In two dimensions one finds for the number of rectangular parallelograms:

$$N(X, Y)\mathrm{d}X\mathrm{d}Y = A\sigma^4 [(L-X)(L-Y)]^2 \times \exp\{-\sigma[L(X+Y)+2XY]\}\,\mathrm{d}X\mathrm{d}Y \quad (3)$$

where A is the area of the medium and σ the surface density of the lines in either the x or the y direction.

The next step is to integrate Equations 2 and 3 over the full range $(0, L)$ of the boundary-variables, X, Y, Z, subject to some constraint on X, Y, Z. This will be in three dimensions:

$$XYZ = v\,(\text{volume of PPP})$$

so as to obtain the volume distribution F_{vol} (vL^{-3}) of fragments. Shape distributions can be further obtained by renaming the variables x, y, z according to their magnitude by X_1, X_2, X_3 such that:

$$X_1 \leqslant X_2 \leqslant X_3,$$

and defining shape-parameters:

$$S_1 \equiv (X_3 - \bar{X})/2\bar{X} \quad (4)$$

$$S_2 \equiv (\bar{X} - X_1)/\bar{X} \quad (5)$$

where $\bar{X} = \frac{1}{3}(X_1 + X_2 + X_3)$. S_1 and S_2 take values between 0 and 1 and measure, respectively, the prolateness and oblateness of the PPP. $F_{\mathrm{pro}}(S_1)$ and $F_{\mathrm{obl}}(S_2)$ are their distribution functions. These S-parameters are connected to those in the Zingg classification system [1, 13] through the relations:

$$\frac{\text{thickness}}{\text{breadth}} = \frac{1-S_2}{(3/2)+S_2-S_1}$$

$$\frac{\text{breadth}}{\text{length}} = \frac{(3/2)+S_2-S_1}{(1/2)+S_1}$$

Another interesting quantity is the volume, $\theta(\rho)V$, that is occupied by PPP, the complement $(1-\theta)V$ being made up of more complex figures. Clearly $\theta(\rho)$ increases with ρ (Fig. 3), it being very small for small ρ when only few of the closed forms are PPP, first rises towards unity as ρ increases, overshoots by about 10% (since the volume of a PPP inside a larger PPP is overcounted), then settles down. Although only a tiny fraction of all the figures are PPP even for moderate ρ (e.g. for $\rho' = \rho L^3 = 0.8$, $\theta = 6.8 \times 10^{-6}$, see Fig. 3), it is very likely that the small bodies are overwhelmingly PPP. This is almost evident for $\rho \sim 0$ (we thank Professor M. Aizenman for pointing this out to us) and for $\rho L^3 \sim 1$ (*a fortiori*, since then almost all figures are PPP).

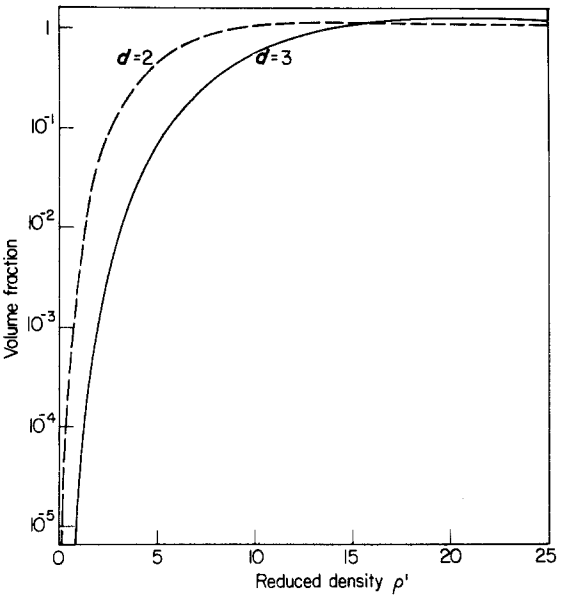

Figure 3 The fraction, θ, of the total space occupied by small regular fragments as a function of the reduced boundary density, ρ'. ρ' is ρL^3 in three dimensions and σL^2 in two dimensions. (L is the linear dimension of plaquettes and of lines forming the boundary.)

In two dimensions one has the distributions $f_{\mathrm{ar}}(aL^{-2})$ for the areas:

$$a \equiv XY$$

as well as the distribution function, $f_{\mathrm{elong}}(S_3)$, for the elongation variable

$$S_3 = \frac{|X-Y|}{X+Y} \quad (6)$$

3. Results

The computed distributions are definite integrals that are probably expressible in terms of known or tabulated functions (indeed $f_{\mathrm{ar}}(a)$ is certainly such). Even so, it was thought more economic to evaluate several distributions simultaneously by a Monte-Carlo procedure involving about 10^6 events.

Typical computed results are shown in Figs. 4 and 5 for two and three dimensions, respectively. The size distribution (being the number of small regular fragments of a given size per unit interval of size) decreases fast with "size" (volume v, for $d = 3$ and area a, for $d = 2$) but, for most of the range, does so slower than exponentially. The shape distributions (defined as the total number of fragments having a given value of the shape

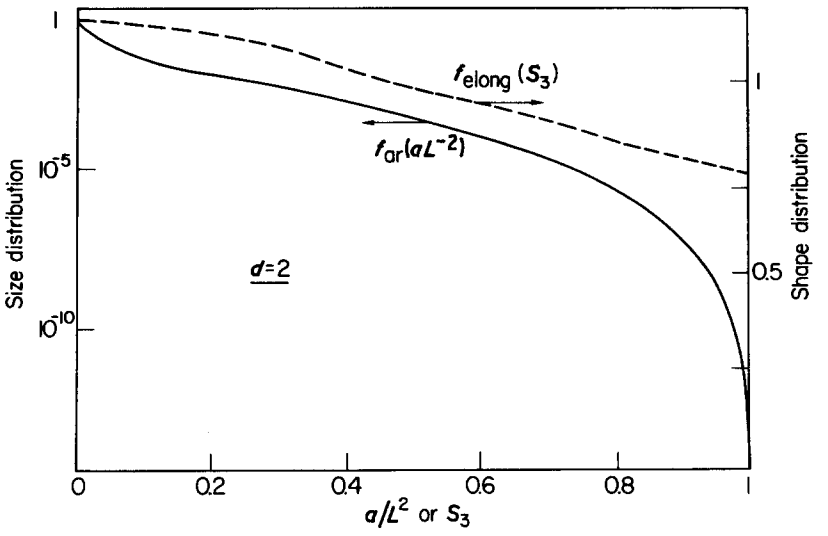

Figure 4 Computed results in two dimensions ($\rho' = 0.4$). Number of fragments per unit area as a function of fragment area: full lines; left hand, logarithmic scale. Number of fragments per unit shape-parameter (Equation 6) as a function of shape parameter: broken lines; right hand, linear scale. (Normalizations: curves on linear scale integrate to unity. Unit of area: L^2.)

parameter S per unit interval or the shape parameter) show a broad coverage of shapes. This situation is common to all densities investigated in this study.

More useful quantities than the distribution function are the cumulative fractions $F_{cum}(vL^{-3})$ and $f_{cum}(aL^{-2})$, defined as the fractional number of all small regular fragments, which are such that their sizes exceed v or a. For v or a equal to zero the cumulative fraction is evidently unity, whereas it is zero for $v = L^3$ or $a = L^2$, these being the largest dimensions of our small regular fragments. According to an empirical law ("the Mott distribution") the cumulative fraction decreases exponentially with the linear dimension of the fragment [3]. Our results have been

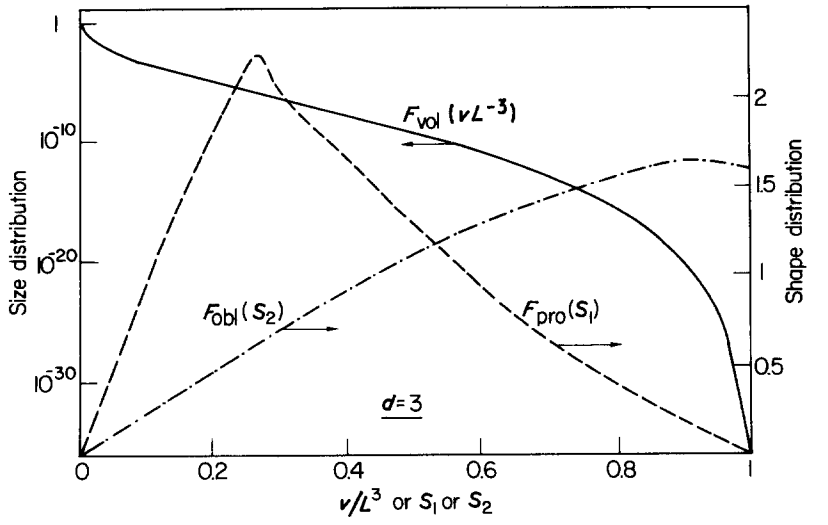

Figure 5 Results in three dimensions (computed for $\rho' = 0.8$). Number of fragments per unit volume as a function of fragment volume: full lines; left hand, logarithmic scale. Number of fragments per unit shape-parameter as a function of shape parameters (Equations 4 and 5): right hand, linear scale. Prolateness (S_1), broken lines; Oblateness (S_2), dash-dotted lines. (Normalizations: curves on linear scale integrate to unity. Unit of volume: L^3.)

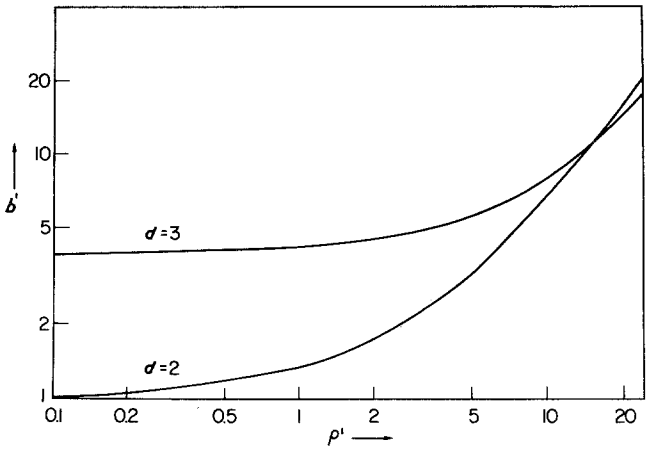

Figure 6 The coefficient b' in the exponent of Equation 7 plotted logarithmically against the reduced density, ρ' (appearing in Fig. 3).

fitted to the forms:

$$\begin{aligned} F_{\text{cum}}(vL^{-3}) &= \exp\left[-b'(\rho')L^{-1}v^{1/3}\right. \\ &\quad \left.-a'(\rho')L^{-3}v\right] \\ f_{\text{cum}}(aL^{-2}) &= \exp\left[-b'(\rho')L^{-1}a^{1/2}\right. \\ &\quad \left.-a'(\rho')L^{-2}a\right] \end{aligned} \tag{7}$$

where ρ' is the dimensionless density of boundaries: ρL^3 and σL^2 in three and two dimensions, respectively.

The coefficient a' measures the deviation from a Mott distribution. It was found that the above fit is an excellent representation of the computed results in two dimensions and a good representation in three dimensions for 99% or more of the fragments.

The coefficient $b(\rho')$ is shown in Fig. 6 as function of the reduced density, ρ'. For a Mott distribution ($a' = 0$) in d-dimensions, b is related to the mean size $\bar{v}_d$ of the fragments through

$$b'/L = (d!/\bar{v}_d)^{1/d}$$

so that $\bar{a} = 2(L/b')^2$ for $d = 2$ and $\bar{v} = 6(L/b')^3$ for $d = 3$. The monotonic increase of b' is in accord with the decrease of the mean size of fragments as the crack density ρ' increases. In the asymptotic range of large densities the term with a' becomes of marginal importance and the above results for the means are exact.

The other coefficient a' in Equation 7 shows an interesting behaviour, in that it changes sign as the crack density increases (Fig. 7). A positive (negative) value of a' gives a distribution that for relatively larger sizes decreases with size faster (slower) than a Mott distribution, so that a log-plot of the cumulative fraction against the linear dimension of the fragments will deviate downwards (upwards). It is convenient to use as a benchmark for fragment distribution that value of ρ' for which $a'(\rho')$ vanishes and the fragments follow a Mott distribution. Naming this value ρ'_{Mott}, our data yield

$$\begin{aligned} \rho'_{\text{Mott}} &= 6 \text{ for } d = 2 \\ &= 9 \text{ for } d = 3. \end{aligned}$$

Experimentally derived fragment-size distributions [5, 6, 14] deviate downwards from the

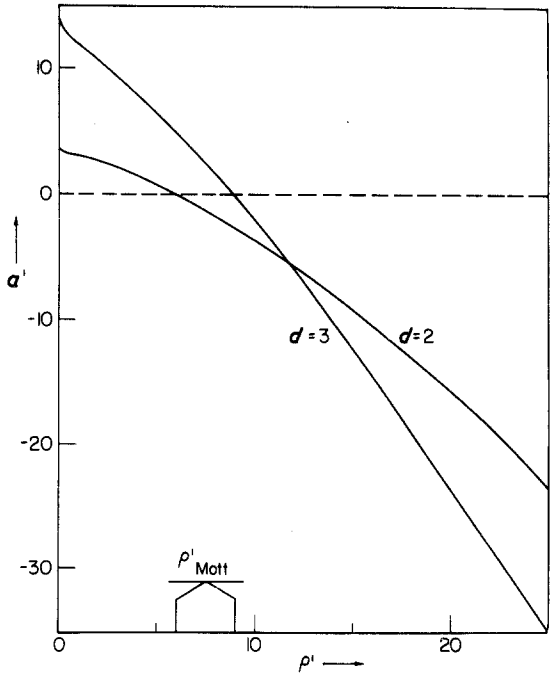

Figure 7 The coefficient a' plotted against ρ' (linear plot). Note the change in the sign of a' at the values ρ'_{Mott} shown by arrows.

Mott distribution, so one would conclude from the model that the experimental crack densities are lower than the Mott-density ρ'_{Mott}.

It appears difficult to formulate a convincing explanation for this phenomenon. The need for further experimental, numerical and theoretical research on this point is one of the consequences of the present investigation.

4. Conclusion

The main outcome of this research is the representation, in parametric form, of the cumulative fragment distributions in two and three dimensions, as shown in Equation 7 and Figs. 4 to 7. The computations establish the Mott distribution ($a' \equiv 0$ in Equation 7) as a standard for the cumulative distribution, from which deviations are expected to occur: significantly, in both directions.

The model of small parallelopipeds is intended as a simplified representation of small fragments. Its virtues are the results it yields and that it is amenable to interesting extensions, such as the effect of dynamical stresses on the fragment distributions or the calculation of the amount of damage in the fragments due to internal cracks present in them [15].

Acknowledgements

Thanks are due to Yishai Levanon and Avi Levi for comments. This research was partly supported by the Directorate of Geoscience Research at the Ministry of Energy and Infrastructure, Jerusalem.

References

1. W. R. BECHTELL, US Army Engineer Waterways Experiment Station, Livermore, Report No. E-75-2 (1975).
2. D. A. SHOCKEY, D. R. CURRAN, L. SEAMAN, J. T. ROSENBERG and C. F. PETERSEN, *Int. J. Rock Mech. Sci. and Geomech. Abstr.* **11** (1974) 303.
3. N. F. MOTT and E. H. LINFOOT, "A theory of fragmentation", Advisory Council on Scientific Research and Technical Development, AC 3348, SD/FP 67 (1943).
4. J. DEHN, "Probability formulas for describing fragment size distributions", US Army Armament Research and Development Command, Aberdeen Proving Ground, Maryland; Technical Report No. ARBRL-TR-2332 (June, 1981).
5. H. C. RODEAU, *Geophysics* **30** (1963) 616.
6. H. M. STERNBERG, "Fragment weight distribution from naturally fragmenting cylinders loaded with various explosives", Naval Ordinance Lab., White Oak, Maryland, NOLTR 73-83, AD-772, 480 (1973).
7. J. K. DIENES, "On the inference of crack statistics from observations of an outcropping", in 20th US Symposium on Rock Mechanics, edited by K. E. Gray *et al.* (University of Texas, Austin, 1979).
8. M. G. KENDALL and P. A. P. MORAN, "Geometrical Probability" (Griffin, London, 1963).
9. A. SPRECHER, private communication (1983).
10. M. AIZENMAN, J. CHAYES, L. CHAYES, J. FRÖHLICH and L. RUSSO, to be published.
11. P. C. ROBINSON, *J. Phys. A: Math. Gen.* **16** (1983) 605.
12. J. M. POLATTY, B. J. HOUSTON, R. L. STONE and D. C. BANKS, US Army Corps of Engineers, Vicksburg, PNE-5003 (1965).
13. F. J. PETTIJOHN, "Sedimentary Rocks" (Harper, New York, 1957).
14. A. D. SOLEM, M. SHAPIRO and B. N. SINGLETON, Jr, "Explosives comparison for fragmentation effectiveness", US Naval Ordinance Lab., White Oak, Maryland, NAVORD 2933 (1953).
15. R. ENGLMAN, Z. JAEGER and A. LEVI, *Phil. Mag.* (1984) in press.

Received 28 December 1983
and accepted 13 March 1984